ORIGINAL ARTICLE

Journal of Research in Dental and Maxillofacial Sciences

DOI: 10.66224/jrdms.11.2. 136

In Vitro Study of Sustained Release Potential and IGF/PDGF Profile of Lyophilized Decellularized Bovine Bone Scaffolds After Freeze-Dried Secretome Application

Firman Fath Rachmadhan [1], David Buntoro Kamadjaja [2], Reza Al Fessi [2]

[1] Clinical Medicine Magister Study Programme, Faculty of Dental Medicine, Universitas Airlangga, Surabaya 60132, Indonesia.
[2] Department of Oral and Maxillofacial Surgery, Faculty of Dental Medicine, Universitas Airlangga, Surabaya 60132, Indonesia.

Corresponding author:
David Buntoro Kamadjaja, Department of Oral and Maxillofacial Surgery, Faculty of Dental Medicine, Universitas Airlangga, Surabaya 60132, Indonesia

david-b-k@fkg.unair.ac.id

Article History
Received: 11 Aug 2025
Accepted: 30 Jan 2026

Abstract

Background and Aim: Craniomaxillofacial bone defects are commonly reconstructed using bovine bone scaffolds, where stable growth factor release is critical for effective bone regeneration. This study investigated the release profile of insulin-like growth factor (IGF) and platelet-derived growth factor (PDGF) from deproteinized bovine bone mineral (DBBM), freeze-dried bovine bone (FDBB), and decellularized freeze-dried bovine bone (dc-FDBB) scaffolds following application of freeze-dried secretome.

Materials and Methods: In this in vitro experimental study, scaffolds were first immersed in secretome and incubated at 4°C for 24 hours to facilitate absorption, followed by an optional freeze-drying step. After rehydration, the release kinetics of IGF and PDGF was measured at 1, 8, 24, and 48 hours using ELISA. Comparisons were made with one-way ANOVA followed by the Tukey's HSD test (alpha=0.05).

Results: FDBB scaffolds treated with freeze-dried secretome exhibited the highest and most sustained release of IGF over 48 hours compared to other groups (26.774±4.079 ng/mL; P<0.05); while PDGF release was generally lower in freeze-dried groups compared to controls (8.587±2.184 ng/mL; P=0.197).

Conclusion: The results showed that freeze-drying influences the release profile of IGF and PDGF and its sustainability from secretome-loaded bovine bone scaffolds, with potential implications for optimizing scaffold bioactivity in bone tissue engineering applications.

Keywords: Insulin-Like Growth Factor I; Platelet-Derived Growth Factor; Secretome; Tissue Scaffolds

Cite this article as: Rachmadhan FF, Kamadjaja DB, Al Fessi R. In Vitro Study of Sustained Release Potential and IGF/PDGF Profile of Lyophilized Decellularized Bovine Bone Scaffolds After Freeze-Dried Secretome Application. **J Res Dent Maxillofac Sci. 2026; 11(2):136-147.**

Introduction

Craniomaxillofacial bone defects due to trauma, infection, congenital anomalies, or surgical resections remain a critical challenge in reconstructive surgery, as they are characterized by substantial loss of bone volume and compromised structural integrity and function [1,2]. Successful reconstruction in this region is particularly demanding due to the need to restore both biomechanical stability and esthetic appearance, as well as to support complex functions such as mastication, speech, and facial expression [3–5]. Autologous bone grafts, harvested from intraoral or extraoral donor sites, are widely recognized as the gold standard for treating such defects [6,7]. They provide osteogenic, osteoinductive, and osteoconductive properties, which are essential for bone regeneration. However, despite their clinical efficacy, autografts are limited by donor site morbidity, restricted graft volume, prolonged surgical time, and the potential for unpredictable resorption, all of which underscore the need for alternative biomaterials [8,9].

Xenogenic bone substitutes, particularly bovine-derived scaffolds, have attracted considerable interest as a viable alternative due to their wide availability, structural similarity to human bone, and their capacity to promote bone regeneration [10,11]. Bovine bone scaffolds retain critical components of the native bone matrix, including both organic and inorganic fractions, which confer osteoconductive and osteoinductive properties. Nevertheless, the biological performance of these scaffolds is highly dependent on the employed processing techniques [12,13]. For example, deproteinized bovine bone mineral (DBBM) involves extensive removal of organic components, yielding a stable mineral phase that supports osteoconduction but may exhibit diminished osteoinductivity [14,15]. Freeze-dried bovine bone (FDBB), in contrast, preserves a higher proportion of bioactive organic constituents, potentially enhancing osteoinductive potential but at the expense of retaining immunogenic residues [16,17]. Decellularized freeze-dried bovine bone (dc-FDBB) represents a further refinement, whereby decellularization techniques are applied to reduce immunogenicity while maintaining extracellular matrix components and the natural bone microarchitecture. Importantly, the incorporation of lyophilization (freeze-drying) as a stabilization method plays a dual role: it safeguards thermo-sensitive proteins and structural features of the scaffold while preserving bioactive molecules crucial for orchestrating regenerative processes [16,18,19].

In parallel with the development of scaffold processing methods, regenerative medicine has increasingly emphasized the role of biological cues in directing bone healing. In this context, the mesenchymal stem cell (MSC)-derived secretome has emerged as a promising therapeutic tool [20,21]. Unlike cell-based therapies that face challenges related to cell survival, immunogenicity, and regulatory concerns, secretome-based strategies provide a cell-free alternative capable of delivering a complex repertoire of bioactive molecules. The secretome comprises cytokines, chemokines, growth factors, and extracellular vesicles that collectively regulate cellular recruitment, angiogenesis, osteogenesis, and immunomodulation [22,23]. Among these components, insulin-like growth factor (IGF) and platelet-derived growth factor (PDGF) have received particular attention for their synergistic roles in bone regeneration. PDGF is primarily active during the early phases of healing, promoting angiogenesis, fibroblast recruitment, and extracellular matrix remodeling [24,25]. Conversely, IGF contributes to sustained

osteoblast proliferation, differentiation, and matrix mineralization, thereby supporting the long-term consolidation and maturation of new bone tissue [24,26].

The integration of secretome with bovine-derived scaffolds offers an innovative approach to enhance scaffold bioactivity while maintaining their structural and mechanical advantages. Supplementing scaffolds with secretome followed by lyophilization, not only stabilizes these bioactive molecules but also enables controlled release over time, a critical factor for orchestrating sequential stages of bone healing [22,27]. However, the influence of different scaffold processing methods—DBBM, FDBB, and dc-FDBB—on the release kinetics and preservation of secretome-derived growth factors has not yet been comprehensively evaluated.

Therefore, the present study was designed to investigate the release profile of IGF and PDGF from bovine bone scaffolds after secretome supplementation and freeze-drying. By elucidating how scaffold processing influences the delivery and bioavailability of these growth factors, this research aimed to provide mechanistic insights into scaffold–secretome interactions and to advance the optimization of xenogenic biomaterials. Ultimately, the findings are expected to contribute to the development of more effective strategies for craniomaxillofacial bone defect reconstruction, bridging the gap between scaffold engineering and biological stimulation for enhanced tissue regeneration

Materials and Methods

This in vitro, experimental study was conducted in accordance with the Declaration of Helsinki and approved by the Health Research Ethical Clearance Commission of the Faculty of Dental Medicine, Universitas Airlangga, No. 0972/HRECC.FODM/IX/2024. This in vitro experimental study employed a longitudinal design, dividing samples into six groups: (1) DBBM + secretome (control), (2) FDBB + secretome (control), (3) dc-FDBB + secretome (control), (4) DBBM + secretome, freeze-dried, (5) FDBB + secretome, freeze-dried, and (6) dc-FDBB + secretome, freeze-dried. The research took place at the Faculty of Pharmacy Universitas Airlangga, from September to November 2024.

Sample size calculation:

The sample size was calculated using the Federer (resource equation) approach, where (n−1) (t−1) must be at least 15; n is the number of samples per group, and t is the number of experimental groups (treatments) [28]. In this study, t=6, therefore 5(n−1)≥15, resulting in n≥4. Accordingly, four samples were included in each group.

Preparation of bone scaffolds:

1. DBBM: It was obtained from the National Research and Innovation Agency of Indonesia, made of bovine cancellous bone (5×5×5 mm blocks), chemically cleaned with 3% hydrogen peroxide, rinsed, then deproteinized by heating at 1000°C, dried (≤10% water), packed, and sterilized by gamma irradiation.
2. FDBB: It was obtained from the National Research and Innovation Agency of Indonesia, made of bovine femur blocks (5×5×5 mm), cleaned as above, underwent freeze-drying at -80°C using Lyovapor™ L-250 (Buchi, Essen, Germany) until water content reached <10%, and then sterilized by gamma irradiation.
3. dc-FDBB: FDBB was obtained from the National Research and Innovation Agency of Indonesia, with an additional decellularization step using sodium lauryl ether sulfate after freeze-drying, then packed and sterilized by gamma irradiation.

Secretome preparation:

Human umbilical cords (donors <40 years, elective caesarean section, no comorbidities) were obtained from the Stem Cell Institute, ITD Universitas Airlangga. The preparation was done according to a previously described method [17,18]. The tissue was enzymatically digested with collagenase IV and DNAase I, cultured in α-MEM + 10% fetal bovine serum (Gibco BRL, Gaithersburg, MD, USA) [29], epidermal growth factor, penicillin/streptomycin, and glutamine (Merck KGaA, Darmstadt, Germany), under standard conditions (5% CO_2, 37°C) in an incubator (Memmert, Brussels, Belgium). The cells were validated by immunocytochemistry using positive (CD105, CD90, CD73) and negative (CD45, CD14, CD34) markers (Biolegend, California, USA), and expanded to passage. After reaching 80% confluence, the cells were shifted to serum-free medium for 48 hours to collect secretome. The supernatant was centrifuged at 407 g for 5 minutes and 1,630 g for 3 minutes, aliquoted, and stored at -20°C (GEA, Dusseldorf, Germany) until use.

Scaffold-secretome application and freeze-drying:

Each scaffold block was immersed in 400 µL of secretome and incubated for 24 hours (37°C, 98% humidity, 5% CO_2). In freeze-dried groups, the scaffolds were subsequently freeze-dried at -80°C. All scaffolds were then rehydrated with 5 mL of phosphate-buffered saline (PBS; Merck KGaA, Darmstadt, Germany) and stored at -20°C in a freezer until use.

Growth factor release assay:

DBBM, FDDB, and dc-FDDB were randomly chosen to be incubated in PBS under standard conditions (5% CO_2, 37°C). At time points of 1, 8, 24, and 48 hours post-rehydration, PBS supernatant was sampled for quantification of released IGF and PDGF using enzyme-linked immunosorbent assay (ELISA) kits (Bioassay Technology Laboratory, Zhejiang, China). Absorbance was read at 450 nm.

Statistical analysis:

Data analysis included using the Shapiro-Wilk test for normality assessment and Levene's test for evaluation of variance homogeneity to confirm the assumptions for parametric analysis. Accordingly, one-way ANOVA was applied to detect between-group differences, followed by Tukey's HSD test when significant ($P<0.05$) to control for type I error in multiple comparisons. When normality was met, but variances were unequal, the Welch's ANOVA was performed, followed by an appropriate post-hoc test for unequal variances (Games–Howell test), when applicable. When the normality assumption was not met, the Kruskal–Wallis test was used, with Dunn's multiple-comparison test applied when required.

For repeated measures across different time points, repeated-measures ANOVA was applied to detect within-group changes over time, and when pairwise comparisons were required, the Bonferroni-adjusted paired t-test was used to reduce the risk of type I error. The analysis was conducted using GraphPad Prism version 9.0.2 (GraphPad, CA, USA).

In addition to P-values, effect sizes were reported where appropriate to support the interpretation of the findings. This experimental in vitro study was not based on a priori power calculation because reliable prior effect size estimates were not available; therefore, sample size adequacy was justified using the Federer (resource equation) approach.

Results

IGF release profile:

The IGF release profile across different scaffold groups at each time point is summarized in Table 1, and the individual IGF release profile across different time points is illustrated in Figure 1.

At 1 hour, the mean amount of released IGF (ng/mL) was the highest in the dc-FDBB freeze-dried group (18.973±2.777 ng/mL), followed by the FDBB freeze-dried (18.375±3.084 ng/mL) and DBBM freeze-dried (15.977±0.973 ng/mL) group. The control values ranged from 12.307 to 18.579 ng/mL. Data were normally distributed and homogeneous; one-way ANOVA revealed significant differences among the groups (P<0.05). The Tukey's post-hoc HSD test showed significant differences between dc-FDBB freeze-dried vs. FDBB control (P=0.025), FDBB freeze-dried vs. FDBB control (P=0.044), and FDBB freeze-dried vs. DBBM control (P=0.036) groups.

At 8 hours, the median IGF level across the groups ranged from 11.866 to 21.773 ng/mL. Due to non-normal distribution of data in the dc-FDBB freeze-dried group, the Kruskal-Wallis test was applied, showing no significant difference (P=0.057). At 24 hours, the mean level of released IGF was the highest in the dc-FDBB freeze-dried group (22.930±2.043 ng/mL), followed by the FDBB freeze-dried (21.458±2.731 ng/mL) and DBBM freeze-dried (20.455±1.891 ng/mL) groups, and the lowest mean IGF levels were observed in the control groups. Normality and homogeneity were confirmed, and ANOVA indicated a significant difference in this regard among the groups (P<0.05). Significant differences were found between several groups including dc-FDBB freeze-dried and FDBB control (P=0.001). At 48 hours, the freeze-dried FDBB group showed the highest release (26.774±4.079 ng/mL), followed by the DBBM freeze-dried (21.741±1.250 ng/mL) and dc-FDBB freeze-dried (20.276±1.146 ng/mL) group. Controls had lower mean values. Data normality was confirmed; however, variance was heterogeneous, leading to the use of Welch's ANOVA, which found no significant difference among the groups (P≥0.05).

PDGF release profile:

The PDGF release profile across different scaffold groups at each time point is summarized in Table 2, and the individual PDGF release profiles across different time points are illustrated in Figure 2. At 1 hour, the mean amount of released PDGF ranged from 7.421±2.111 ng/mL in dc-FDBB freeze-dried group to 8.804±0.270 ng/mL in the dc-FDBB control group. Normal distribution and homogeneity were confirmed, and ANOVA showed no significant difference (P=0.793). At 8 hours, the mean values ranged from 6.986±0.246 ng/mL (dc-FDBB freeze-dried) to 10.426±1.466 ng/mL (FDBB control). Data were normal but heterogeneous; the Welch's ANOVA indicated no significant difference (P=0.078).

At 24 hours, the mean amount of released PDGF varied between 8.666±1.627 ng/mL and 10.268±0.756 ng/mL with confirmed normality and homogeneity; ANOVA showed no significant difference (P=0.829). At 48 hours, the mean values ranged from 8.587±2.184 ng/mL (DBBM freeze-dried) to 11.266±0.962 ng/mL (FDBB control). Data distribution and variance were normal and homogeneous; ANOVA confirmed no significant difference (P=0.197). These results demonstrate that freeze-drying influenced the sustained release of IGF variably across scaffold types, with FDBB freeze-dried scaffolds showing the highest sustained IGF release at 48 hours. PDGF release, however, showed less variation across groups and time points.

Table 1. IGF release profile in the study groups at 1, 8, 24, and 48 hours

Time	Group	Mean (ng/L)	SD (ng/L)	Shapiro Wilk (p)[a]	Levene's Test (p)[b]	One-way ANOVA (p)[c]
1 hour	dc-FDBB *Secretome Freeze Dried* (n=3)	18.73	2.777	0.106	0.173	**0.021** *
	FDBB *Secretome Freeze Dried* (n=3)	18.375	3.084	0.509		
	DBBM *Secretome Freeze Dried* (n=3)	15.977	0.973	0.524		
	dc-FDBB *Secretome* (n=3)	16.093	1.040	0.744		
	FDBB *Secretome* (n=3)	12.307	1.996	0.598		
	DBBM *Secretome* (n=3)	18.579	2.178	0.212		
Time	**Group**	**Median (ng/L)**	**Range (ng/L)**	**Shapiro Wilk (p)[a]**	**Levene's Test (p)[b]**	**Kruskal-Wallis (p)[d]**
8 hours	dc-FDBB *Secretome Freeze Dried* (n = 3)	20.638	20.600-22.842	**0.028** *	–	0.057
	FDBB *Secretome Freeze Dried* (n = 3)	20.797	20.578-22.305	0.223		
	DBBM *Secretome Freeze Dried* (n = 3)	20.704	15.128-23.045	0.558		
	dc-FDBB *Secretome* (n = 3)	18.780	15.232-19.295	0.223		
	FDBB *Secretome* (n = 3)	11.866	11.598-17.239	0.080		
	DBBM *Secretome* (n = 3)	21.773	20.808-32.404	0.143		
Time	**Group**	**Mean (ng/L)**	**SD (ng/L)**	**Shapiro Wilk (p)[a]**	**Levene's Test (p)[b]**	**One-way ANOVA (p)[c]**
24 hours	dc-FDBB *Secretome Freeze Dried* (n = 3)	22.930	2.043	0.667	0.135	**0.001** **
	FDBB *Secretome Freeze Dried* (n = 3)	21.458	2.731	0.441		
	DBBM *Secretome Freeze Dried* (n = 3)	20.455	1.891	0.242		
	dc-FDBB *Secretome* (n = 3)	19.168	2.948	0.060		
	FDBB *Secretome* (n = 3)	12.162	1.941	0.249		
	DBBM *Secretome* (n = 3)	17.200	0.405	0.577		
48 hours	dc-FDBB *Secretome Freeze Dried* (n = 3)	20.276	1.416	0.861	**0.019** *	0.072
	FDBB *Secretome Freeze Dried* (n = 3)	26.774	4.079	0.508		
	DBBM *Secretome Freeze Dried* (n = 3)	21.741	1.250	0.790		
	dc-FDBB *Secretome* (n = 3)	18.713	0.913	0.734		
	FDBB *Secretome* (n = 3)	14.661	3.228	0.188		
	DBBM *Secretome* (n = 3)	16.206	5.468	0.112		

[a] P≥0.05 indicates that the data are normally distributed.
[b] P≥0.05 indicates that the variance between groups is homogeneous.
[c] One-way ANOVA if the data meet the requirements for normal distribution in all groups and the variance between groups is homogeneous. One-way Welch's ANOVA if the data meet the requirements for normality, but the variance between groups is not homogeneous.
[d] Reported as median and range (minimum and maximum values); Kruskal-Wallis test if the data do not meet the requirements for normal distribution in all groups.
* P<0.05; ** P<0.01

Table 2. PDGF release profile in the study groups at 1, 8, 24, and 48 hours

Time	Group	Mean (ng/L)	SD (ng/L)	Shapiro Wilk (p)[a]	Levene's Test (p)[b]	One-way ANOVA (p)[c]
1 hour	dc-FDBB *Secretome Freeze Dried* (n = 3)	7.421	2.111	0.732	0.060	0.793
	FDBB *Secretome Freeze Dried* (n = 3)	7.751	1.730	0.154		
	DBBM *Secretome Freeze Dried* (n = 3)	7.906	0.668	0.871		
	dc-FDBB *Secretome* (n = 3)	8.804	0.270	0.555		
	FDBB *Secretome* (n = 3)	8.267	0.545	0.780		
	DBBM *Secretome* (n = 3)	8.381	1.060	0.309		
Time	**Group**	**Median (ng/L)**	**Range (ng/L)**	**Shapiro Wilk (p)[a]**	**Levene's Test (p)[b]**	**Kruskal-Wallis (p)[d]**
8 hours	dc-FDBB *Secretome Freeze Dried* (n = 3)	6.986	0.246	0.921	**0.033***	0.078
	FDBB *Secretome Freeze Dried* (n = 3)	7.554	1.168	0.823		
	DBBM *Secretome Freeze Dried* (n = 3)	7.278	3.168	0.300		
	dc-FDBB *Secretome* (n = 3)	8.697	0.724	0.267		
	FDBB *Secretome* (n = 3)	10.426	1.466	0.929		
	DBBM *Secretome* (n = 3)	8.438	2.006	0.513		
Time	**Group**	**Mean (ng/L)**	**SD (ng/L)**	**Shapiro Wilk (p)[a]**	**Levene's Test (p)[b]**	**One-way ANOVA (p)[c]**
24 hours	dc-FDBB *Secretome Freeze Dried* (n = 3)	9.055	2.911	0.211	0.084	0.829
	FDBB *Secretome Freeze Dried* (n = 3)	9.213	1.031	0.313		
	DBBM *Secretome Freeze Dried* (n = 3)	8.918	0.808	0.467		
	dc-FDBB *Secretome* (n = 3)	8.666	1.627	0.993		
	FDBB *Secretome* (n = 3)	10.268	0.756	0.474		
	DBBM *Secretome* (n = 3)	8.742	1.214	0.952		
48 hours	dc-FDBB *Secretome Freeze Dried* (n = 3)	8.624	1.739	0.632	0.183	0.197
	FDBB *Secretome Freeze Dried* (n = 3)	9.202	0.316	0.571		
	DBBM *Secretome Freeze Dried* (n = 3)	8.587	2.184	0.460		
	dc-FDBB *Secretome* (n = 3)	9.483	1.326	0.786		
	FDBB *Secretome* (n = 3)	11.266	0.962	0.962		
	DBBM *Secretome* (n = 3)	10.548	1.178	0.230		

[a] P≥0.05 indicates that the data are normally distributed.

[b] P≥0.05 indicates that the variance between groups is homogeneous.

[c] One-way ANOVA if the data meet the requirements for normal distribution in all groups and the variance between groups is homogeneous. One-way Welch's ANOVA is used if the data meet the requirements for normality, but the variance between groups is not homogeneous.

* P<0.05; ** P<0.01

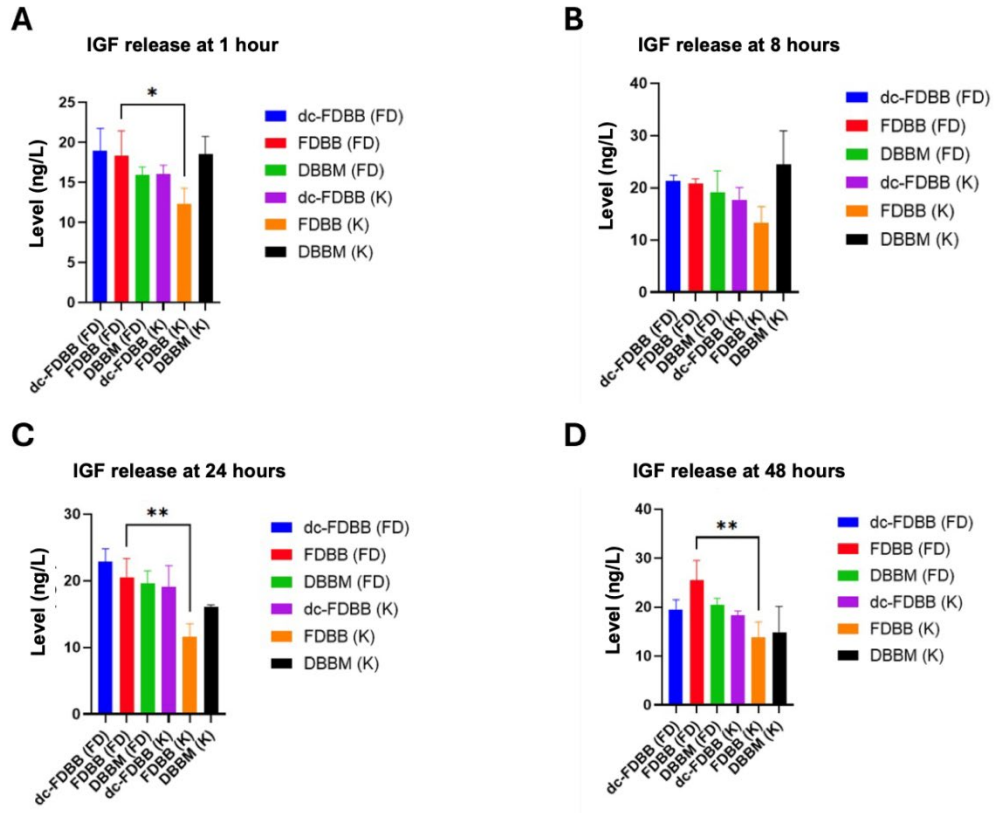

Figure 1. IGF release profile in the study groups at (A) 1 hour, (B) 2 hours, (C) 3 hours, and (D) 4 hours

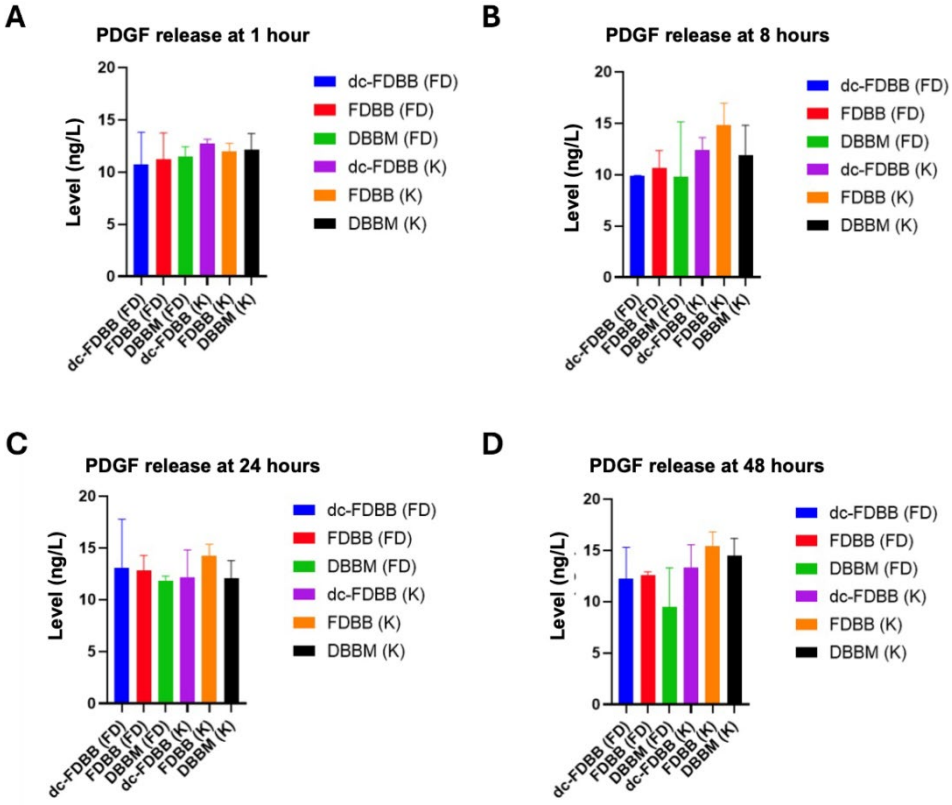

Figure 2. PDGF release profile for each group at (A) 1 hour, (B) 2 hours, (C) 3 hours, and (D) 4 hours

Discussion

This study evaluated the release profile of IGF and PDGF from bovine bone scaffolds processed via deproteinization (DBBM), freeze-drying (FDBB), and decellularization combined with freeze-drying (dc-FDBB), following secretome supplementation with and without lyophilization, monitored over a 48-hour period. The results provide new insights into the influence of scaffold processing and lyophilization on growth factor stabilization and delivery, which are central determinants of scaffold-mediated bone regeneration.

Decellularization effectively reduced immunogenic potential by removing cellular components while retaining critical extracellular matrix constituents, which are indispensable for osteoinduction and preserving the natural bone architecture [16,17]. Freeze-drying further enhanced the bioactivity of scaffolds by stabilizing thermolabile proteins, minimizing hydrolytic degradation, and reducing microbial contamination [30,31]. Together, these processes underscore the importance of balancing structural preservation with biological functionality when designing next-generation xenogenic biomaterials.

Notably, the freeze-dried FDBB secretome group demonstrated the most gradual and sustained release of IGF across the 48-hour observation period. This finding supports the hypothesis that lyophilization contributes to protein stabilization by converting soluble proteins into a solid amorphous state, thereby protecting their tertiary and quaternary structures from hydrolytic cleavage and enzymatic inactivation [24,25]. The sustained IGF availability is particularly significant, given IGF's central role in osteoblast proliferation, matrix synthesis, and mineralization. Predictable release kinetics are critical for maintaining prolonged osteogenic activity and reducing the risk of premature scaffold resorption or incomplete defect healing. In contrast, non-freeze-dried scaffolds, especially DBBM controls, exhibited declining IGF concentrations, indicating compromised protein stability and highlighting the insufficiency of unmodified scaffolds for controlled biofactor delivery [32,33].

Interestingly, PDGF release remained relatively uniform across scaffold types and time points, with DBBM controls demonstrating marginally more stable levels. This profile is consistent with PDGF's recognized role as an early-phase mediator in bone repair, where transient signaling is sufficient to initiate angiogenesis, fibroblast migration, and progenitor cell recruitment [34,35]. Unlike IGF, sustained PDGF release may be less critical, as short-term activity can effectively trigger the cascade of early healing events. This observation aligns with prior evidence suggesting that PDGF serves primarily as a rapid-response growth factor, complementing the prolonged action of osteogenic mediators such as IGF [25].

The complementary release dynamics of IGF and PDGF identified in this study provide a compelling rationale for tailoring scaffold processing methods according to specific regenerative requirements [36]. For instance, scaffolds designed for large or chronic defects, where long-term osteogenesis is critical, would benefit most from freeze-dried FDBB secretome, given its capacity for sustained IGF delivery. Conversely, situations requiring robust early angiogenic and proliferative signaling may allow greater flexibility in scaffold type, as PDGF release was consistent across conditions [37]. These findings underscore the potential of combinatorial or staged scaffold designs to synchronize early vascularization with long-term matrix deposition, thereby optimizing the overall regenerative outcome [16,17].

From a translational perspective, these results highlight the promise of integrating MSC-derived secretome with xenogenic scaffolds as a cell-free

regenerative strategy. Compared with cell transplantation approaches, secretome supplementation offers advantages in terms of safety, scalability, and regulatory acceptance, while still harnessing the paracrine activity of stem cells [20,26]. Moreover, lyophilization as a processing technique adds practical value by enabling storage stability, reduced handling complexity, and the possibility of off-the-shelf clinical products, which are highly desirable in craniomaxillofacial reconstructive settings.

Nevertheless, several limitations should be acknowledged. The present study was conducted under in vitro conditions, which cannot fully replicate the complex cellular, vascular, and mechanical microenvironment of living tissues. Growth factor interactions with immune cells, endothelial cells, and osteoclasts in vivo may substantially modify the release kinetics and regenerative outcomes observed here. Furthermore, the evaluation was restricted to two representative growth factors, whereas the MSC secretome contains a diverse array of cytokines, chemokines, and extracellular vesicles that likely act in concert. Future studies employing in vivo models and multi-omic profiling approaches are warranted to validate scaffold–secretome interactions and to identify the optimal scaffold configurations for clinical translation.

In summary, this study demonstrated that scaffold processing and lyophilization significantly influenced the release kinetics of IGF and PDGF from bovine-derived bone scaffolds. Freeze-dried FDBB secretome scaffolds exhibited superior capacity for sustained IGF release, supporting prolonged osteogenic activity, while PDGF release remained relatively stable across scaffold types, consistent with its role in early-phase healing. These findings provide a foundation for rational scaffold design, where the combination of secretome supplementation and lyophilization may be strategically applied to enhance craniomaxillofacial bone regeneration.

Conclusion

This study showed that IGF release significantly differed among different scaffold groups at 1 and 24 hours; whereas, PDGF release did not. Freeze-dried scaffolds demonstrated a more stable IGF release compared to non-freeze-dried scaffolds. Among the tested groups, freeze-dried FDBB secretome provided the most gradual and sustained IGF release up to 48 hours, while PDGF release remained comparable across scaffolds, with DBBM control exhibiting a relatively stable pattern. Further in vivo studies are needed to confirm scaffold characteristics and identify the optimal option for osteogenesis.

References

1. Chuxi Z, Xinkang Z, Xiaokun D, Shilei Z, Xinrong C. CMF defects database: A craniomaxillofacial defects dataset and a data-driven repair method. Biomed Signal Process Control. 2024 May;91:105939.

2. Verbist M, Vandevelde AL, Geusens J, Sun Y, Shaheen E, Willaert R. Reconstruction of craniomaxillofacial bone defects with 3D-printed bioceramic implants: Scoping review and clinical case series. J Clin Med. 2024 May;13(10): 2805.

3. de Carvalho AB, Rahimnejad M, Oliveira RL, Sikder P, Saavedra GS, Bhaduri SB, et al. Personalized bioceramic grafts for craniomaxillofacial bone regeneration. Int J Oral Sci. 2024 Oct;16(1):62.

4. Dewey MJ, Harley BAC. Biomaterial design strategies to address obstacles in craniomaxillofacial bone repair. RSC Adv. 2021;11(29):17809-27.

5. Zhou Y, You D, Xu M, Shao Y, Hu X, Xie Y, et al. Bionic repair strategy for craniomaxillofacial bone tissue reconstruction. Transl Dent Res. 2025 Jul;1(3):100037.

6. Schmidt AH. Autologous bone graft: Is it still the gold standard? Injury. 2021 Jun;52:S18-22.

7. Robinson PG, Abrams GD, Sherman SL, Safran MR, Murray IR. Autologous Bone Grafting. Oper Tech Sports Med. 2020 Dec;28(4):150780.

8. Gillman CE, Jayasuriya AC. FDA-approved bone grafts and

bone graft substitute devices in bone regeneration. Mater Sci Eng C. 2021 Nov;130:112466.

9. Budiatin AS, Khotib J, Samirah S, Ardianto C, Gani MA, Putri BR, et al. Acceleration of bone fracture healing through the use of bovine hydroxyapatite or calcium lactate oral and implant bovine hydroxyapatite – Gelatin on bone defect animal model. Polymers (Basel). 2022 Nov; 14(22):4812.

10. Widhiyanto L, Utomo DN, Perbowo AP, Hernugrahanto KD. Macroscopic and histologic evaluation of cartilage regeneration treated using xenogenic biodegradable porous sponge cartilage scaffold composite supplemented with allogenic adipose derived mesenchymal stem cells (ASCs) and secretome: An in vivo experiment. J Biomater Appl. 2020 Sep;35(3):422-9.

11. Suyatno A, Nurfinti WO, Kusuma CPA, Pratama YA, Ardianto C, Samirah S, et al. Effectiveness of Bilayer Scaffold Containing Chitosan / Gelatin / Diclofenac and Bovine Hydroxyapatite on Cartilage / Subchondral Regeneration in Rabbit Joint Defect Models. Adv Pharmacol Pharm Sci. 2024;2024(1):6987676.

12. Pratama YA, Ananta IP, Haris MS, Maghfiroh N, Nabila H, Ardianto C, et al. Accelerated bone defect closure after administration of nano bovine hydroxyapatite-calcium sulfate-gelatin scaffold in bone defect models. J Pharm Pharmacogn Res. 2025 Nov;13(6):1728-41.

13. Pratama YA, Marhaeny HD, Deapsari F, Budiatin AS, Rahmadi M, Miatmoko A, et al. Development of Hydroxyapatite as a Bone Implant Biomaterial for Triggering Osteogenesis. Eur J Dent. 2025 May. Epub ahead of print.

14. Zhu YW, Wei YW, Ma JY, Chen W, Shen Z, Qiu J. Bioactive deproteinized bovine bone mineral based on self-assembled albumin nanoparticles promoted bone regeneration via activation of Wnt/β-catenin pathway. Mater Today Bio. 2025 Jun;32:101730.

15. Parisi L, Buser D, Chappuis V, Asparuhova MB. Cellular responses to deproteinized bovine bone mineral biofunctionalized with bone-conditioned medium. Clin Oral Investig. 2021 Apr;25(4):2159-73.

16. Nugraha AP, Kamadjaja DB, Sumarta NPM, Rizqiawan A, Pramono C, Yuliati A, et al. Osteoinductive and osteogenic capacity of freeze-dried bovine bone compared to deproteinized bovine bone mineral scaffold in human umbilical cord mesenchymal stem cell culture: An in vitro study. Eur J Dent. 2023 Oct;17(4):1106-13.

17. Vidarta RP, Kamadjaja DB, Danudiningrat CP, Amir MS, Rizqiawan A, Yuliati A, et al. Degradation rate and weight loss analysis for freeze-dried, decellularized, and deproteinized bovine bone scaffolds. Dent J. 2025 Mar;58(1):23-9.

18. Sahetapy OM, Kamadjaja DB, Danudiningrat CP, Rizqiawan A. Comparative study of biomechanical characteristics of deproteinized and decellularized bovine bone block scaffold. J Int Dent Med Res. 2025 May;18(2):594-8.

19. Bracey DN, Jinnah AH, Willey JS, Seyler TM, Hutchinson ID, Whitlock PW, et al. Investigating the osteoinductive potential of a decellularized xenograft bone substitute. Cells Tissues Organs. 2019 Nov;207(2):97-113.

20. El Moshy S, Radwan IA, Rady D, Abbass MM, El-Rashidy AA, Sadek KM, et al. Dental stem cell-derived secretome/conditioned medium: The future for regenerative therapeutic applications. Stem Cells Int. 2020;2020(1):7593402.

21. Iaquinta MR, De Pace R, Benkhalqui A, D'Agostino A, Trevisiol L, Finotti A, et al. Secretome release during in vitro bone marrow-derived mesenchymal stem cell differentiation induced by Bio-Oss® collagen material. Int J Mol Sci. 2025 Apr;26(8): 3807.

22. Perwira FD, Utomo DN, Widhiyanto L, Hernugrahanto KD. Physiobiochemical and microbiologic stability characteristics of freeze-dried cartilage secretome Adipose Mesenchymal Stem Cell (AdMSC). Int J Health Sci (Qassim). 2022;6(S5):7584-93.

23. Trigo CM, Rodrigues JS, Camões SP, Solá S, Miranda JP. Mesenchymal stem cell secretome for regenerative medicine : Where do we stand ? J Adv Res. 2025 Apr;70:103-24.

24. Putra ZK, Mahyudin F, Suroto H. Comparison of five growth factors in the secretomes of hypoxic bone marrow mesenchymal stem cells and hypoxic adipose mesenchymal stem cells. Bali Med J. 2024 Jan;13(1):577-81.

25. Cecerska-Heryć E, Goszka M, Serwin N, Roszak M, Grygorcewicz B, Heryć R, et al. Applications of the regenerative capacity of platelets in modern medicine. Cytokine Growth Factor Rev. 2022 Apr;64:84-94.

26. Prado-Yupanqui JW, Ramírez-Orrego L, Cortez D, Vera-Ponce VJ, Chenet SM, Tejedo JR, et al. The hidden power of the secretome: Therapeutic potential on wound healing and cell-free regenerative medicine—A systematic review. Int J Mol Sci. 2025 Feb;26(5):1926.

27. Nur A, Putri K, Rizqiawan A, Amir MS. Preosteoblast adhesion and viability study of freeze-dried bovine bone block

scaffold coated with human umbilical cord mesenchymal stem cell secretome. Eur J Dent. 2025 Feb;19(01):197-205.

28. Charan J, Kantharia N. How to calculate sample size in animal studies? J Pharmacol Pharmacother. 2013 Dec;4(4):303-6.

29. Cheng L, Liu J, Wang Q, Hu H, Zhou L. The protective effect of a human umbilical cord mesenchymal stem cell supernatant on UVB-induced skin photodamage. Cells. 2024;13(2):156. doi:10.3390/cells13020156.

30. Merivaara A, Zini J, Koivunotko E, Valkonen S, Korhonen O, Fernandes FM, et al. Preservation of biomaterials and cells by freeze-drying: Change of paradigm. J Control Release. 2021 Aug;336:480-98.

31. Fu JN, Wang X, Yang M, Chen YR, Zhang JY, Deng RH, et al. Scaffold-based tissue engineering strategies for osteochondral repair. Front Bioeng Biotechnol. 2022 Jan;9:812383.

32. Feng J, Meng Z. Insulin growth factor-1 promotes the proliferation and osteogenic differentiation of bone marrow mesenchymal stem cells through the Wnt/β-catenin pathway. Exp Ther Med. 2021 Aug;22(2):891.

33. Wang S, Umrath F, Cen W, Reinert S, Alexander D. Angiogenic potential of vegf mimetic peptides for the biofunctionalization of collagen/hydroxyapatite composites. Biomolecules. 2021 Oct;11(10):1538.

34. Wang Z, Zhu P, Li H, Ye B, Luo Q, Cheng J, et al. Sodium hyaluronate-PDGF repairs cartilageand subchondral bone microenvironment via HIF-1α-VEGF-notch and SDF-1-CXCR4 inhibitionin osteoarthritis. J Cell Mol Med Orig. 2025 Apr;29(7):e70515.

35. Xu J, Wang Y, Li Z, Tian Y, Li Z, Lu A, et al. PDGFRα reporter activity identifies periosteal progenitor cells critical for bone formation and fracture repair. Bone Res. 2022 Jan;10(1):7.

36. Ashraf S, Burston JJ, Shahtaheri M, McWilliams DF, Chapman V, de Moor CH, et al. Osteocyte phenotypes in human and monoiodoacetate-induced rat osteoarthritis. Osteoarthr Cartil. 2022 Apr;30:S319.

37. Lerner UH, Kindstedt E, Lundberg P. The critical interplay between bone resorbing and bone forming cells. J Clin Periodontol. 2019 Jun;46:33-51.